Recurrent thyroid cancer with changing histologic features

S. Michelle Shiller, DO, Kartik Konduri, MD, Leeanne K. Harshman, MD, Brian J. Welch, MD, and John C. O'Brien Jr., MD

We present the case of a 57-year-old woman diagnosed with breast cancer and a thyroid mass that was suspicious for cancer. The breast cancer was estrogen and progesterone receptor negative, HER2/neu borderline, with a high proliferative index. Treatment of this cancer took precedence. Nine months later, a total thyroidectomy was done for papillary thyroid cancer with metastases to 2 of 8 perithyroid lymph nodes. Postoperative radioactive iodine ablation was given. Recurrent thyroid disease was found in the right neck 1 year later and was resected; no radioactive iodine was given at that time. After 2½ years, the cancer recurred as a more highly aggressive, undifferentiated anaplastic thyroid carcinoma. Treatment is discussed.

In June 2009, a 57-year-old woman presented with a mass in the lower midline of the neck. Sonographic findings at that time included an enlarging hypoechoic lesion adjacent to the left thyroid bed and enlarging right jugular chain nodes. A computed tomography (CT) scan in July 2009 showed new and enlarging soft tissue densities in the thyroid resection bed bilaterally, possibly representing recurrent tumor, and extensive bilateral cervical lymphadenopathy, with a 2-cm midline necrotic node. A fine-needle aspiration (FNA) biopsy in August 2009 revealed undifferentiated carcinoma that, based on immunohistochemical stains, was compatible with metastatic thyroid carcinoma *(Figure 1)*.

The patient's past medical history was significant for prior thyroid cancer and breast cancer. She had originally presented with a tender mass on the right side of the neck in May 2006. An FNA of this mass in the right upper pole of her thyroid was suspicious for thyroid cancer. However, she was also diagnosed with cancer of her left breast, the treatment of which took precedence. A modified radical mastectomy was done, and pathologic examination showed infiltrating ductal carcinoma, moderate to poorly differentiated with medullary features, with a 1.2-cm invasive component (pT1c, pN0, pMX). The breast cancer was an aggressive type: an estrogen receptor/progesterone receptor negative, HER2/neu borderline tumor with a high proliferation index. The axillary dissection removed 12 lymph nodes, all of which were negative for metastatic carcinoma. After the mastectomy, the patient underwent four cycles of doxorubicin/cyclophosphamide chemotherapy followed by

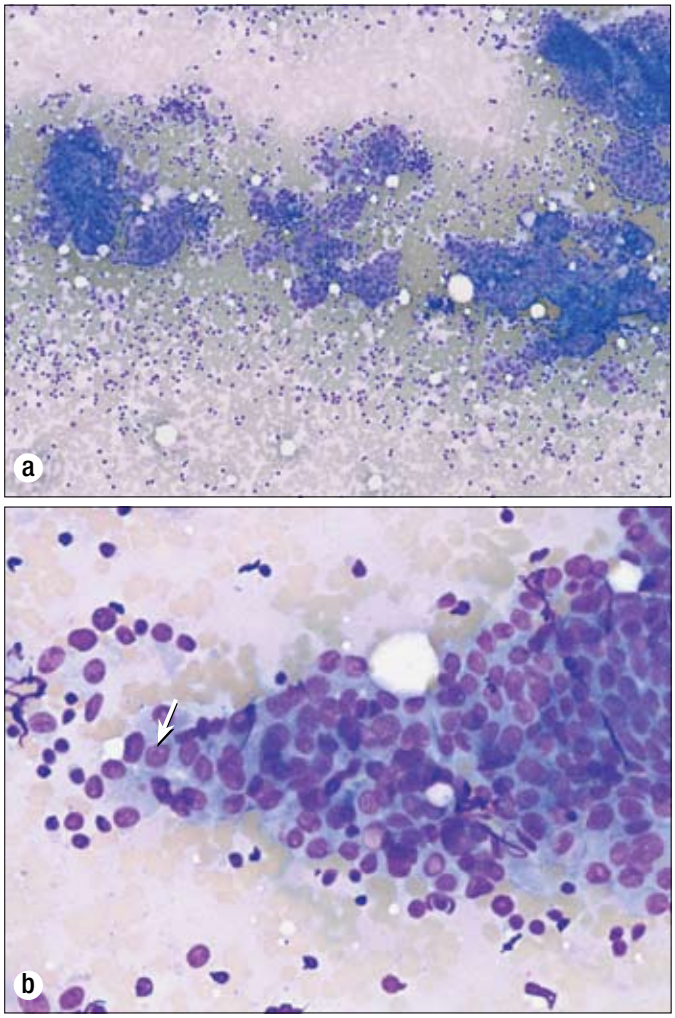

Figure 1. Biopsy results in 2006. **(a)** Cytologic preparation with the Diff-Quik stain method demonstrates sheets of cells in a papillary configuration. 40×. **(b)** A higher-power view of sheets of cells with an increased nuclear to cytoplasmic ratio, conspicuous nucleoli (arrow), and occasional nuclear grooves. Diff-Quik stain, 100×.

From the Departments of Pathology (Shiller), Oncology (Konduri), Nuclear Radiology (Harshman), Endocrinology (Welch), and Surgery (O'Brien), Baylor University Medical Center at Dallas and Baylor Sammons Cancer Center, Dallas, Texas.

Corresponding author: S. Michelle Shiller, DO, Department of Pathology, Baylor University Medical Center, 3500 Gaston Avenue, Dallas, Texas 75246 (e-mail: Shirley.Shiller@BaylorHealth.edu).

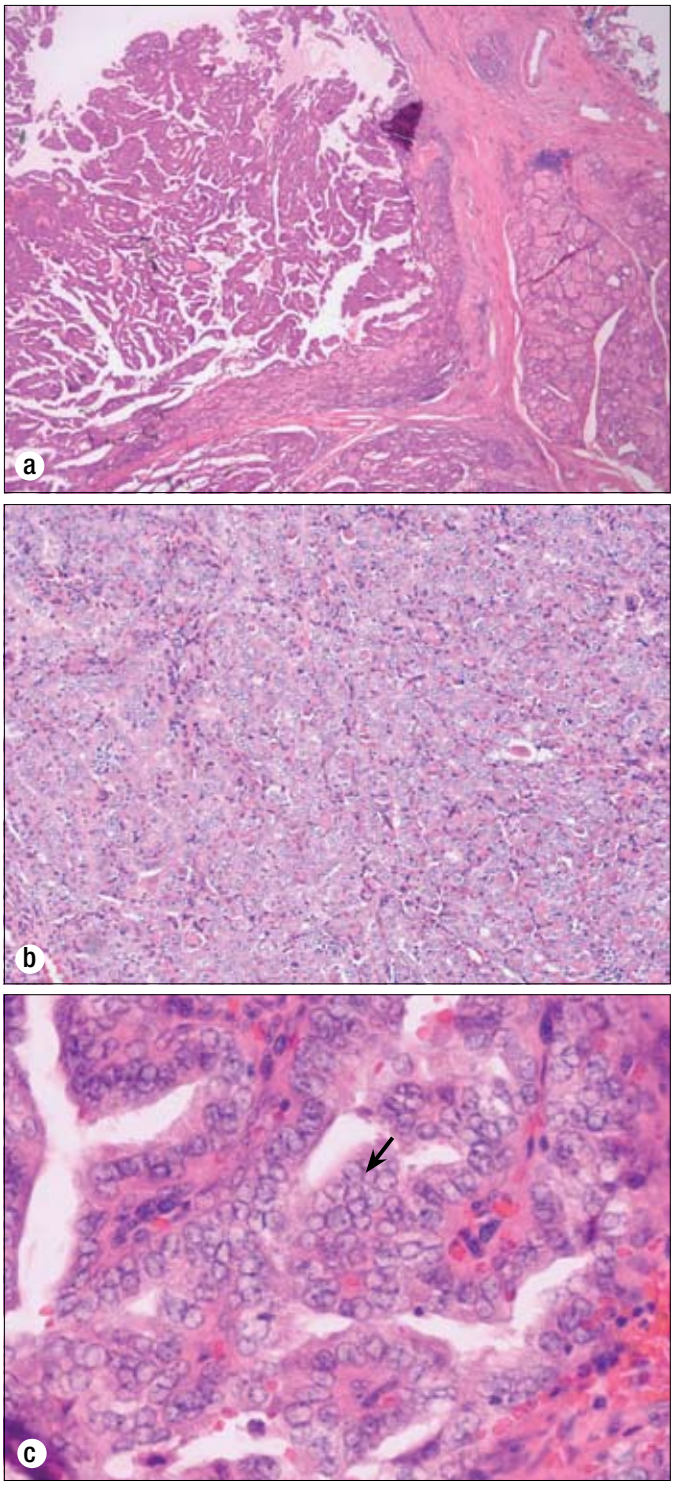

Figure 2. Biopsy results of the thyroid gland in 2007 showing papillary carcinoma. **(a)** A focus of well-differentiated papillary thyroid carcinoma. Hematoxylin and eosin stain (H&E), 40×. **(b)** Fibrovascular cores and clear nuclei. H&E, 100×. **(c)** Conspicuous nucleoli, clear chromatin, and nuclear grooves (arrow). H&E, 400×.

four cycles of docetaxel. These treatments were completed in December 2006.

A frozen section of the right lobe of the thyroid in February 2007 revealed papillary carcinoma. A total thyroidectomy was done. Pathologic examination showed multifocal papillary carcinoma (with the largest nodule measuring 2.4 cm),

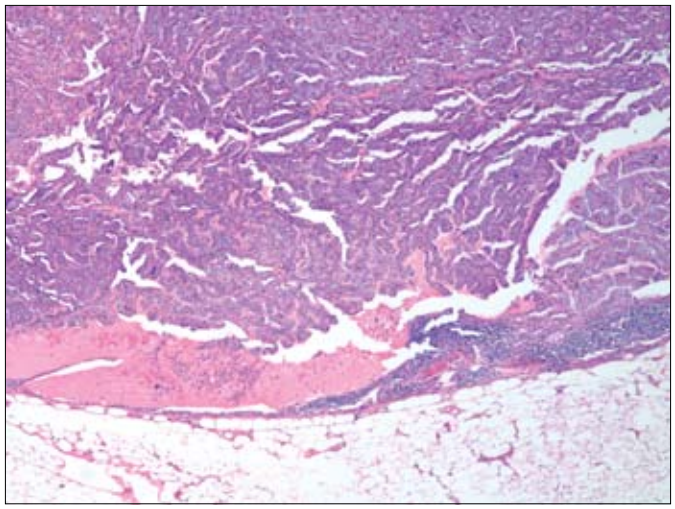

Figure 3. Perithyroidal lymph node with metastatic papillary carcinoma in 2007. Two of eight lymph nodes were positive for metastatic disease in the original resection. H&E, 100×.

metastases to two of eight perithyroid nodes, and involvement of the perinodal and perithyroid soft tissue (T3, N1a, MX, stage III) *(Figures 2 and 3).* In May 2007, the patient received postoperative treatment with 150 mCi of radioactive iodine (RAI^{131}). The posttreatment body scan showed uptake in the thyroid bed and in level II nodes in the right side of the neck. She was placed on 150 mcg of levothyroxine daily.

In August 2007, a sonogram showed a mass on the right side of the neck. Another sonogram in November 2007 showed a 3-cm mass in the right level II area. A CT scan in November 2007 showed the tumor with surrounding subcentimeter-enhancing nodes concerning for metastases and possible mediastinal lymphadenopathy. An FNA biopsy of this mass was diagnosed as metastatic papillary thyroid carcinoma in January 2008, and it was resected in February 2008. Pathology showed a 2.5 × 1.5 × 1.5–cm metastasis of papillary carcinoma with perinodal soft tissue involvement.

A sonogram in May 2008 found three lymph nodes adjacent to the right thyroid bed measuring approximately 1 cm each. During this time (January to May), the patient's unstimulated thyroglobulin had decreased from 45 to 5 ng/mL, and her antithyroglobulin antibodies were negative. The plan was to continue to follow the thyroglobulin levels and repeat sonograms. The thyroglobulin decreased to 4.9 in September 2008 and to 3.9 in June 2009. Thyrogen-stimulated whole body scan was recommended, but the patient elected to wait.

In June 2009, a sonogram of the neck found a 3.2-cm mass in the left central neck, a 1.8-cm mass on the right between the common carotid artery and the internal jugular vein, and enlarging right jugular chain adenopathy. A CT scan of the neck in July 2009 showed new soft tissue involvement in the left thyroid resection bed and enlarging soft tissue masses in the right thyroid resection bed, which likely represented recurrent thyroid cancer *(Figure 4).* This CT also demonstrated extensive bilateral metastatic cervical lymphadenopathy, with a 2-cm midline necrotic lymph node. FNA of a pretracheal mass was diagnosed as metastatic poorly differentiated carcinoma *(Figure 5).*

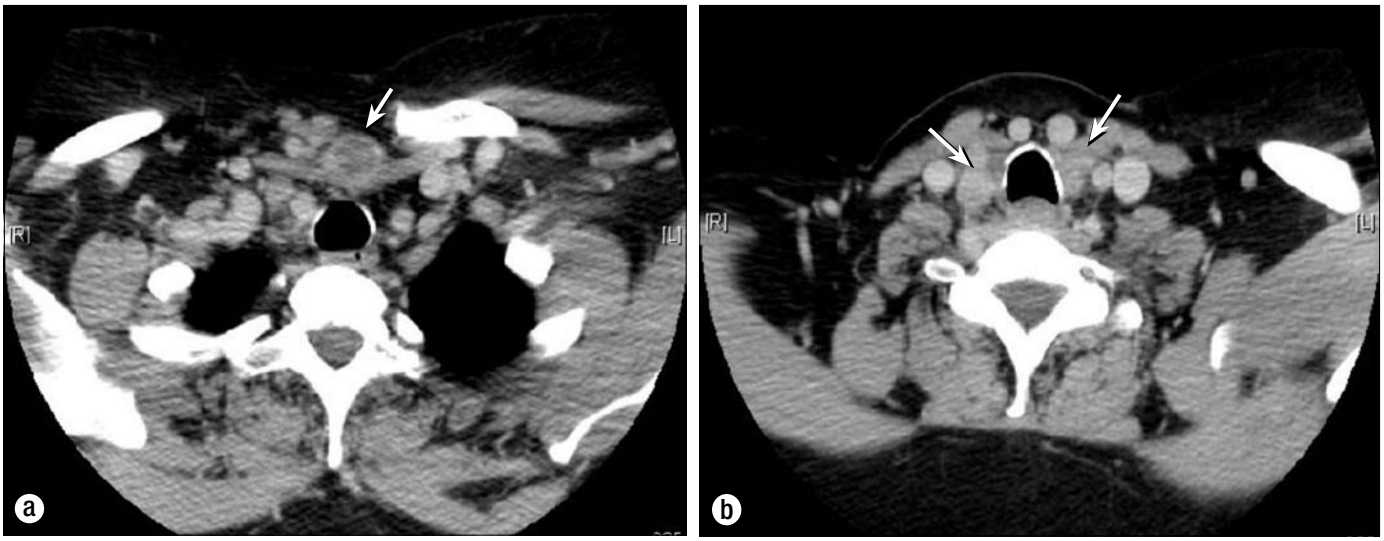

Figure 4. CT scan in September 2009 showing (**a**) a necrotic suprasternal mass (arrow) penetrating through the sternothyroid/sternohyoid muscles and **(b)** the extent of bilateral disease in the thyroid bed (arrows).

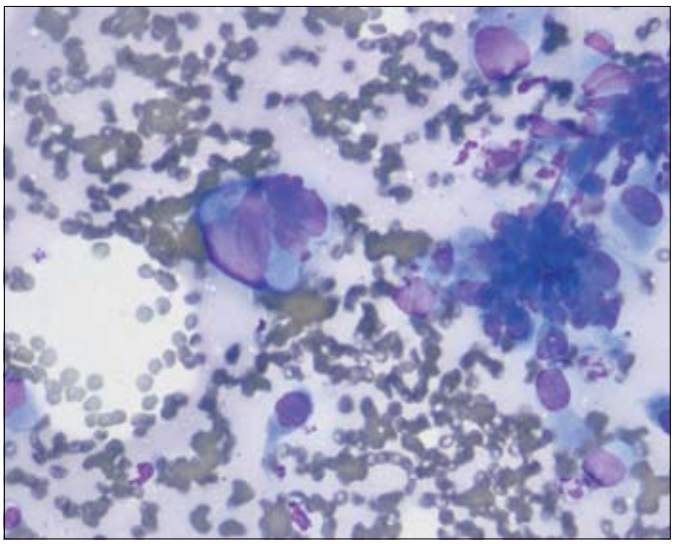

Figure 5. Fine-needle aspiration completed in early August 2009 showing marked nuclear atypia, increased nuclear to cytoplasmic ratio, and occasional nuclear grooves, diagnosed as metastatic poorly differentiated carcinoma. Diff-Quik, 100×.

The patient was referred to the senior author (JCO), and on September 14, 2009, she underwent a direct laryngoscopy (which showed good movement in both vocal cords), bilateral selective neck dissections, resection of recurrent disease in the central compartment, and bilateral paratracheal node dissections using the Xomed nerve integrity monitor *(Figure 6).* The dissection extended inferiorly to the brachiocephalic vein in the mediastinum. The right recurrent laryngeal and vagus nerves and the internal jugular vein were resected due to involvement with cancer. The left recurrent laryngeal nerve was preserved even though cancer was dissected from the area between the nerve and the esophagus. The left superior parathyroid was identified and left *in situ.* Postresection laryngoscopy showed an immobile right vocal cord and a fully mobile left cord. One hour after surgical resection, the patient began experiencing respiratory stridor and was taken back to the operating room for an emergency tracheostomy. The skin was sutured to the tracheotomy incision to prevent spillage of tracheal secretions into the neck dissection wounds.

Multiple pathological specimens were examined. Overall, in the bilateral selective neck dissections, 29 lymph nodes were identified, 9 of which were positive for metastatic carcinoma (right side: 5/10 level III nodes and 2/4 level IV nodes; left side: 0/8 level III nodes and 2/7 level IV nodes) *(Figure 7).* Additionally, invasive undifferentiated carcinoma was present in the tissue surrounding the right recurrent laryngeal nerve and multiple nodules within the central compartment dissection. Extensive lymphovascular invasion was present. A varying histologic spectrum was present, including well-differentiated papillary thyroid carcinoma as well as undifferentiated (anaplastic) carcinoma *(Figure 8).* Immunohistochemical studies in papillary thryoid carcinoma are routinely positive for TTF-1 and thyroglobulin, and such analysis in this case supported the diagnosis of metastatic thyroid carcinoma *(Figure 9).* Of note, thyroglobulin was expressed in the well-differentiated components of the metastatic tumor, but not

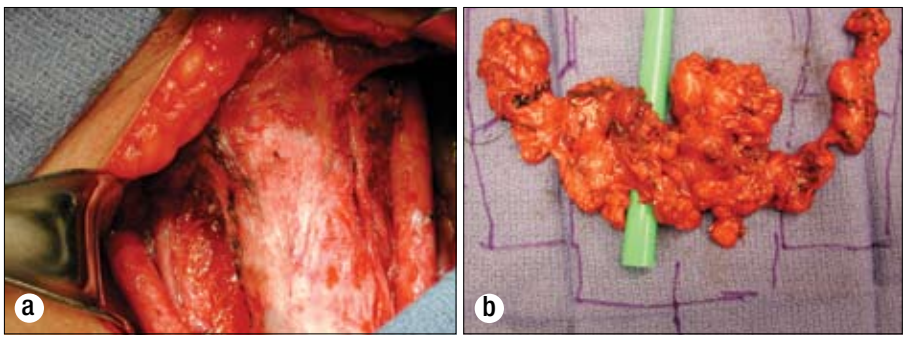

Figure 6. The September 2009 surgery. (**a**) The postresection thyroid bed. **(b)** Specimens.

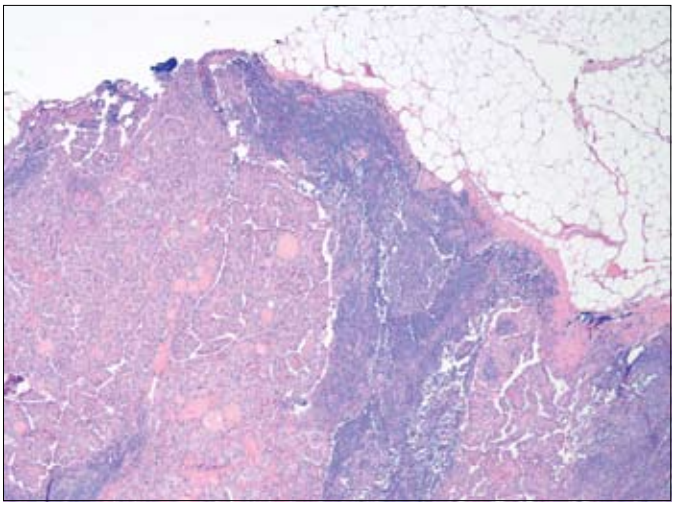

Figure 7. Representative metastatic lymph node with area of papillary carcinoma from September 2009 selective neck dissection. H&E, 40×.

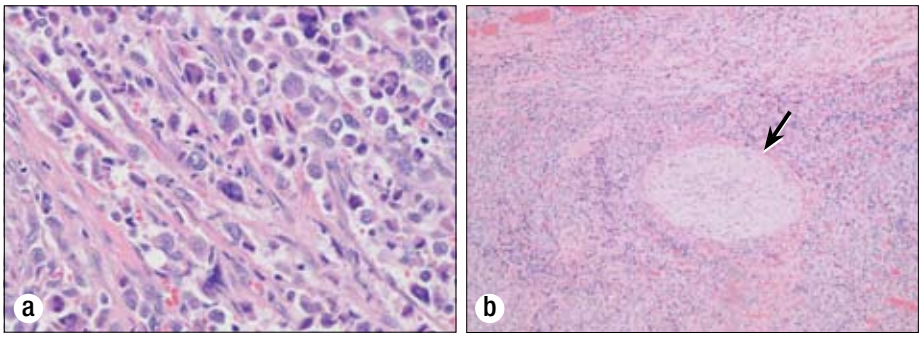

Figure 8. (a) Metastatic carcinoma with anaplastic features. H&E, 400×. **(b)** Perineural entrapment (arrow)/invasion by anaplastic thyroid carcinoma. H&E, 40×.

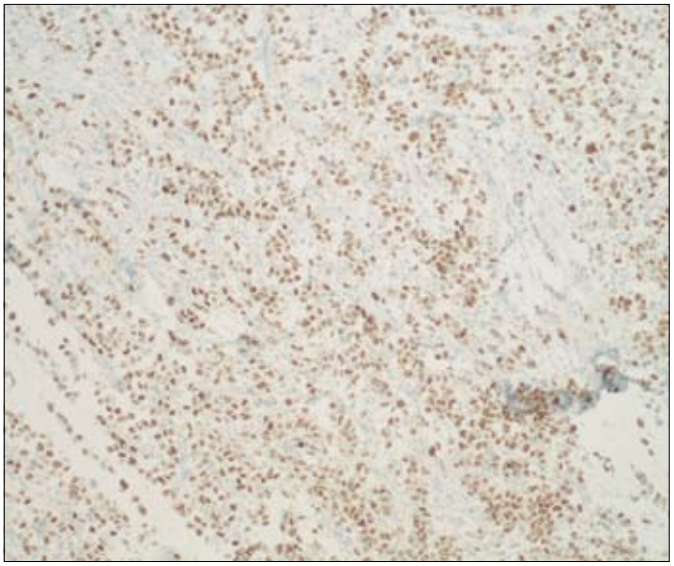

Figure 9. Immunohistochemical stain positive for TTF-1 in undifferentiated/anaplastic cells. 100×.

in the undifferentiated areas. Surgical margins were negative; the anterior subcutaneous margin was the closest at 1 mm (T4b, N1b, MX, stage IVB).

Postoperatively, the patient recovered well. She was treated with supplemental intravenous calcium for several days due to hypocalcemia but was then switched to an oral calcium supplementation. Her parathyroid hormone and calcium levels returned to normal before discharge. The tracheostomy tube was downsized and later capped. A dysphagiagram showed no aspiration, and she was given a soft diet. Her incision healed well, and she was discharged home 1 week after surgery.

Positron emission and computed tomography scans (PET/CT) on September 29, 2009, showed a single millimetric hypermetabolic focus abutting the right side of the laryngeal cartilage but no evidence of distant disease *(Figure 10)*. While this single focus was worrisome for locally persistent thyroid carcinoma, additional differential considerations included a small reactive lymph node.

Adjuvant therapy with radioactive iodine 200 mCi RAI^{131} was given on October 6, 2009, 3 weeks after resection, when her thyroid-stimulating hormone level was elevated >40 mIU/mL. A posttreatment whole-body scan 7 days later revealed uptake in the posterior aspect of the right lobe of the liver, midabdominal uptake thought to be inferior to the pancreas, and virtually no uptake in the neck *(Figure 11)*. This study did not show the focus in the right neck near the larynx and did show possible liver metastasis that the PET did not show. To delineate the abdominal disease further, a CT of the abdomen was performed on October 15, 2009. This exam showed multiple hepatic low-density lesions, some of which were indeterminate given subcentimeter size, and some of which were determined to be fluid attenuation and thus cystic in nature *(Figure 12)*. The largest was a 3.1-cm lesion in the posterior segment of the right hepatic lobe, which correlated to the area of uptake on the I-131 whole-body scan. Additionally, this abdominal CT showed questionable wall thickening of the third portion of the duodenum, possibly correlating to the area of uptake inferior to the pancreas on the I-131 whole-body scan. Magnetic resonance imaging (MRI) of the abdomen on October 27, 2009, showed multiple hepatic cysts, the largest in the area of the lesion found on the RAI study *(Figure 13)*. This MRI revealed no abnormality within the mid

Figure 10. PET imaging from September 2009 demonstrates physiologic distribution of fluorodeoxyglucose (FDG) accumulation throughout the imaged body. Incidental note is made of partial dose infiltration at the right antecubital injection site. A tiny focus of increased FDG uptake was present in the right neck abutting the laryngeal cartilage but was not well visualized on the maximum-intensity projection (MIP) image.

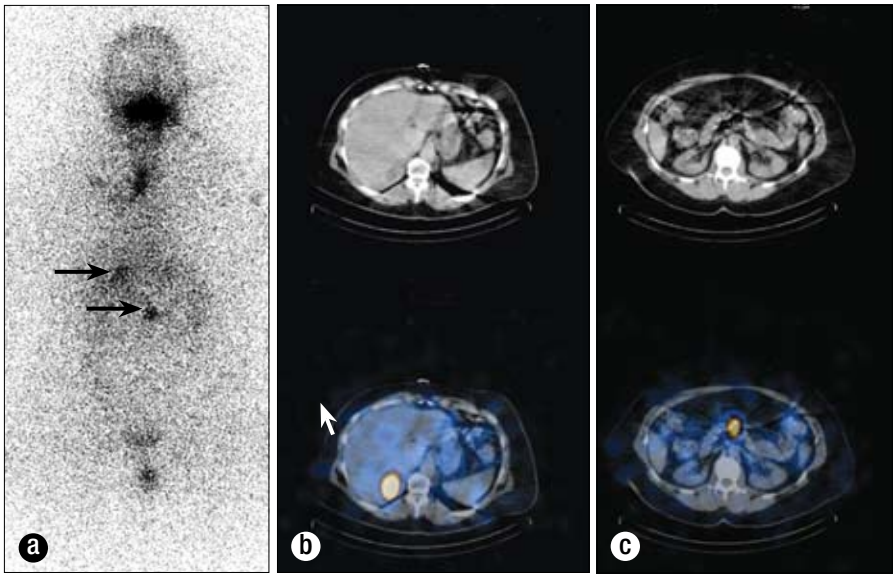

Figure 11. Whole-body I-131 scintigraphy study of October 13, 2009. **(a)** The anterior image demonstrates a region of intense increased radiotracer accumulation in the right upper quadrant, projecting over the liver (arrow). A second region of moderate increased radiotracer accumulation is located within the midabdomen, located slightly inferior to the previously described right upper quadrant activity (arrow). The vertical increased radiotracer accumulation at the neck was confirmed to reflect activity at the patient's tracheostomy site on single photon emission computed tomography (SPECT) consistent with inflammatory-type tracer uptake. Physiologic tracer accumulation was also identified in the mouth and urinary bladder. **(b)** Fusion images through the liver demonstrate that the round region of increased I-131 tracer accumulation corresponds to a low-density right hepatic lobe lesion on CT localization images. **(c)** Images through the midabdomen demonstrate a region of increased I-131 tracer accumulation located at the level of the inferior pancreas, without a definite correlate on CT localization images.

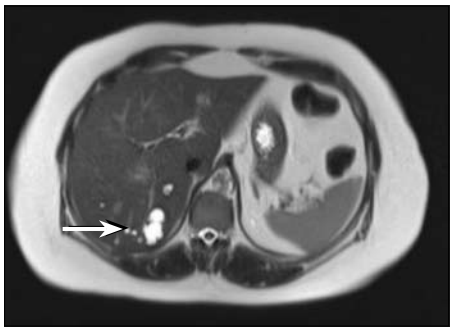

Figure 13. Transaxial T2-weighted image from a magnetic resonance study of the abdomen performed on October 27, 2009, demonstrates a fluid-signal lesion in the right posterior hepatic lobe with some internal septations, consistent with a complex cyst (arrow). This corresponds to the region of abnormal I-131 tracer accumulation as well as the low-density hepatic lesion on the abdominal CT scan.

abdomen to correlate to the abnormal I-131 tracer accumulation located inferior to the pancreas. The I-131 tracer accumulation in the posterior right hepatic lobe on I-131 whole-body imaging thus correlated to a hepatic cyst on both diagnostic abdominal CT and MR scans. Several case reports in the literature have documented uptake of I-131 tracer within benign hepatic cysts on whole-body imaging, thus mimicking a functional thyroid carcinoma metastasis (1, 2). The exact physiologic mechanism is unknown but may be secondary to slow exchange of molecules between cysts and the liver parenchyma itself (1).

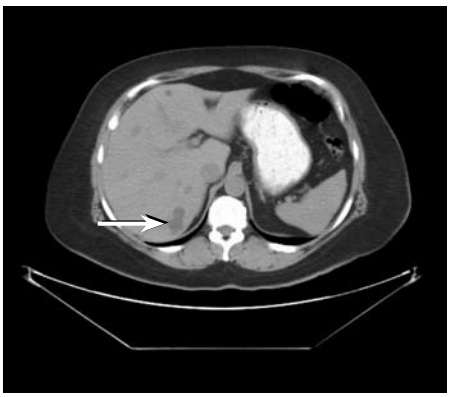

Figure 12. CT of the abdomen without contrast performed on October 15, 2009, demonstrates a lobulated, low-density right posterior hepatic lobe lesion (arrow) that corresponds to the location of abnormal increased I-131 accumulation on scintigraphy. This lesion measures fluid density. A few other millimetric low-density lesions are noted within the liver on this transaxial image, too small to characterize.

After RAI treatment in October 2009, the patient was placed on levothyroxine, with a goal of keeping the thyroid-stimulating hormone level <0.1 mIU/mL. In addition, she received a sensitizing dose of 10 mg/m^2 doxorubicin weekly for 5 weeks concurrently with intensity-modulated radiation therapy (IMRT) to the involved areas.

A follow-up PET/CT on February 25, 2010, demonstrated interval resolution of the focus of hypermetabolism abutting the right thyroid cartilage seen on the earlier PET/CT. The February 2010 exam showed development of a new, small focus of hypermetabolism along the left paratracheal laryngeal musculature adjacent to some surgical clips. There was no correlate on CT images, and the hypermetabolism was thought to reflect muscular activation, although a metastasis could not be entirely excluded. Some hypermetabolic pulmonary opacities had also developed consistent with postradiation pneumonitis.

DISCUSSION

Over a short 2½-year period of time, our patient progressed from having well-differentiated papillary thyroid carcinoma to a mix of papillary and anaplastic carcinoma. Cancer with anaplastic variants may arise from Hurthle cell variants of follicular carcinomas or other similar types of papillary thyroid cancer. Histologic transformations can result in the very aggressive variant of anaplastic thyroid cancer. About 20% of patients with anaplastic carcinoma have had a prior differentiated thyroid cancer, and 20% to 30% have coexisting well-differentiated and anaplastic disease (3–7).

The transition to a less-differentiated type is a very poor prognostic factor. While the usual papillary thyroid cancer is not aggressive, with a 10-year survival of 80% to 90%, the more rare anaplastic thyroid cancer has a 5-year disease-specific mortality rate near 100%. The survival time after diagnosis is usually <6 months (8). Outcomes for anaplastic thyroid cancer are the same regardless of whether an antecedent cancer was present (4, 5).

Molecular models of thyroid carcinogenesis show a variety of mutations *(Table),* but the loss of the p53 tumor suppressor gene

Table. Oncogenes and tumor suppressor genes in thyroid tumors

Neoplasm	Contributory genetic abnormalities	Genetic abnormalities of uncertain importance
Autonomously functioning thyroid nodule	TSH receptor–activating mutation; Gs-α mutation decreasing GTPase activity	
Nodular goiter (colloid nodules)	Many nodules are monoclonal, but precise gene abnormalities are unknown	
Follicular adenoma	*RAS* mutations	c-myc and c-fos overexpressed; *PTEN* abnormalities
Papillary thyroid carcinoma	*BRAF* (V600E) activating mutation; *RET* rearrangements *(RET/PTC)*; *NTRK1* rearrangements *(TRK)*; 14q13.3 and 5q34 (pre-mir-146a)	Tumor suppressor hypermethylation; miRNA upregulation; *TIMM44* mutations
Follicular thyroid carcinoma	*PAX8-PPARγ1* fusion; *RAS* activating mutations	Tumor-specific LOH throughout genome
Anaplastic thyroid carcinoma	*P53* mutations; *BRAF* (V600E) activating mutation; exon 3 *CTNNB1* mutations	*PIK3CA*
Medullary thyroid carcinoma	*RET* activating mutations	

Reprinted with permission from Malchoff, 2009 (11).

TSH indicates thyroid-stimulating hormone; LOH, loss of heterozygosity.

appears to lead to anaplastic transformation (9–11). This case seems to follow the pattern outlined by Quiros and colleagues (12), in which papillary thyroid carcinoma can transform to anaplastic thyroid carcinoma when a p53 mutation occurs after the initial *BRAF* mutation. The p53 mutation is the most common genetic change identified in neoplasia; it is also evident in breast cancer (which this patient also had).

To date, aggressive chemotherapy treatment approaches have not been effective in anaplastic thyroid carcinoma. For local disease in the neck, several reports suggest a survival advantage with a combination of radiotherapy and chemotherapy. This was the approach used in our patient. In a small study of 55 patients, concurrent chemotherapy with doxorubicin and radiation resulted in a 9% 2-year survival rate (13). In another study, patients who underwent potentially curative neck exploration had a median survival of 43 months compared with 3 months with palliative resection. Of the eight patients who had potentially curative surgery and received postoperative chemotherapy and irradiation, four survived longer than 2 years (14). Chemotherapy with paclitaxel-containing regimens has been shown to have response rates of around 50% for advanced/metastatic anaplastic thyroid cancers. Median survival was 24 weeks with this drug (15). Other drugs including platinum agents, mitoxantrone, and vincristine also have some level of efficacy. However, none of these agents result in lasting responses.

Radiation therapy is usually delivered using conformal techniques in the treatment of differentiated and undifferentiated thyroid carcinoma. In this case, IMRT was used. IMRT allows for the delivery of escalating doses of radiation, with the hope of decreasing both short- and long-term side effects. Minimizing side effects is especially important in the treatment of anaplastic thyroid carcinoma, given the concurrent use of doxorubicin, which has marked radiation sensitization ability. M. D. Anderson Cancer Center in Houston, Texas, recently published their series, which found a possible benefit with conformal radiation in "healthy patients" with localized disease who were able to tolerate "full dose irradiation" as well as a survival advantage in the same group of patients who received >50 Gy (16). In addition, Schwartz et al, also from M. D. Anderson, found in their review of the use of conformal radiation therapy in differentiated thyroid carcinoma that the use of IMRT was associated with less frequent severe morbidity but had no impact on survival (17). The risk factors that Schwartz et al found to have a significant effect on survival were high-risk histologic features, M1 disease, and gross residual disease. Unfortunately, our patient had high-risk histologic features (anaplastic thyroid carcinoma), possible microscopic residual disease, and M1 disease by PET. Our patient received >60 Gy to the postoperative bed and sites of potential neck node involvement, with an additional boost using IMRT to the site of PET positivity in the right paralaryngeal cartilage area to the upper 60 Gy range. Particular attention was also paid to the tracheostomy site, which is a common place of recurrence with anaplastic thyroid carcinoma. Our patient tolerated concurrent doxorubicin and radiation therapy reasonably well. Since the patient had prior doxorubicin therapy for her breast cancer, cardiac function was evaluated to monitor her ejection fraction.

Because about half of these patients die due to upper airway obstruction, it is important to secure the airway by the use of tracheostomy and other means. Palliative care should also be an integral part of the treatment approach. The dedifferentiated cells have lost the human sodium-iodide symporter function, so radioiodine therapy is not as efficacious. The RAI treatment in this case was given to treat any residual differentiated cancer cells retaining the capability to absorb iodine and any possible metastases that could do the same.

Antiangiogenic agents including axitinib, antitumor vasculature drugs like combretastin, and gene transfer strategies to affect p53 function are being evaluated in clinical studies for advanced anaplastic thyroid cancer. Several studies have shown that after gene therapy targeting p53, cells were more susceptible to radiation and chemotherapy, tended to redifferentiate, and had reduced proliferation (18–22).

In conclusion, anaplastic thyroid cancer remains a very aggressive malignancy with few effective treatment options. Long-term outcomes for patients with this disease are usually poor. Some new agents are being evaluated in clinical studies.

Total resection of disease with postresection chemotherapy and radiation is associated with the best chance for survival.

Acknowledgments

The authors thank Cynthia Orticio, MA, ELS, for editorial contributions.

1. Okuyama C, Ushijima Y, Kikkawa M, Yamagami T, Nakamura T, Kobayashi K, Hirota T, Nishimura T. False-positive I-131 accumulation in a liver cyst in a patient with thyroid carcinoma. *Clin Nucl Med* 2001;26(3):198–201.
2. Gunawardana DH, Pitman AG, Lichtenstein M. Benign hepatic cyst mimicking a functional thyroid carcinoma metastasis on whole-body I-131 imaging. *Clin Nucl Med* 2003;28(6):527–528.
3. Nel CJ, van Heerden JA, Goellner JR, Gharib H, McConahey WM, Taylor WF, Grant CS. Anaplastic carcinoma of the thyroid: a clinicopathologic study of 82 cases. *Mayo Clin Proc* 1985;60(1):51–58.
4. Carcangiu ML, Steeper T, Zampi G, Rosai J. Anaplastic thyroid carcinoma. A study of 70 cases. *Am J Clin Pathol* 1985;83(2):135–158.
5. Venkatesh YS, Ordonez NG, Schultz PN, Hickey RC, Goepfert H, Samaan NA. Anaplastic carcinoma of the thyroid. A clinicopathologic study of 121 cases. *Cancer* 1990;66(2):321–330.
6. Tan RK, Finley RK 3rd, Driscoll D, Bakamjian V, Hicks WL Jr, Shedd DP. Anaplastic carcinoma of the thyroid: a 24-year experience. *Head Neck* 1995;17(1):41–47.
7. McIver B, Hay ID, Giuffrida DF, Dvorak CE, Grant CS, Thompson GB, van Heerden JA, Goellner JR. Anaplastic thyroid carcinoma: a 50-year experience at a single institution. *Surgery* 2001;130(6):1028–1034.
8. Giuffrida D, Gharib H. Anaplastic thyroid carcinoma: current diagnosis and treatment. *Ann Oncol* 2000;11(9):1083–1089.
9. Fagin JA. Molecular genetics of human thyroid neoplasms. *Annu Rev Med* 1994;45:45–52.
10. Learoyd DL, Messina M, Zedenius J, Robinson BG. Molecular genetics of thyroid tumors and surgical decision-making. *World J Surg* 2000; 24(8):923–933.
11. Malchoff CD. Oncogenes and tumor suppressor genes in thyroid nodules and nonmedullary thyroid cancer. In Basow DS, ed. *UpToDate.* Waltham, MA: UpToDate, 2009.
12. Quiros RM, Ding HG, Gattuso P, Prinz RA, Xu X. Evidence that one subset of anaplastic thyroid carcinomas are derived from papillary carcinomas due to *BRAF* and p53 mutations. *Cancer* 2005;103(11):2261–2268.
13. Tennvall J, Lundell G, Wahlberg P, Bergenfelz A, Grimelius L, Akerman M, Hjelm Skog AL, Wallin G. Anaplastic thyroid carcinoma: three protocols combining doxorubicin, hyperfractionated radiotherapy and surgery. *Br J Cancer* 2002;86(12):1848–1853.
14. Haigh PI, Ituarte PH, Wu HS, Treseler PA, Posner MD, Quivey JM, Duh QY, Clark OH. Completely resected anaplastic thyroid carcinoma combined with adjuvant chemotherapy and irradiation is associated with prolonged survival. *Cancer* 2001;91(12):2335–2342.
15. Ain KB, Egorin MJ, DeSimone PA; Collaborative Anaplastic Thyroid Cancer Health Intervention Trials (CATCHIT) Group. Treatment of anaplastic thyroid carcinoma with paclitaxel: phase 2 trial using ninety-six-hour infusion. *Thyroid* 2000;10(7):587–594.
16. Bhatia A, Rao A, Ang KK, Garden AS, Morrison WH, Rosenthal DI, Evans DB, Clayman G, Sherman SI, Schwartz DL. Anaplastic thyroid cancer: Clinical outcomes with conformal radiotherapy. *Head Neck* 2009 Nov 2 [Epub ahead of print].
17. Schwartz DL, Lobo MJ, Ang KK, Morrison WH, Rosenthal DI, Ahamad A, Evans DB, Clayman G, Sherman SI, Garden AS. Postoperative external beam radiotherapy for differentiated thyroid cancer: outcomes and morbidity with conformal treatment. *Int J Radiat Oncol Biol Phys* 2009;74(4):1083–1091.
18. Kim TH, Lee SY, Rho JH, Jeong NY, Soung YH, Jo WS, Kang DY, Kim SH, Yoo YH. Mutant p53 (G199V) gains antiapoptotic function through signal transducer and activator of transcription 3 in anaplastic thyroid cancer cells. *Mol Cancer Res* 2009;7(10):1645–1654.
19. Lee YJ, Chung JK, Kang JH, Jeong JM, Lee DS, Lee MC. Wild-type p53 enhances the cytotoxic effect of radionuclide gene therapy using sodium iodide symporter in a murine anaplastic thyroid cancer model. *Eur J Nucl Med Mol Imaging* 2009 Sep 1 [Epub ahead of print].
20. Barzon L, Gnatta E, Castagliuolo I, Trevisan M, Moretti F, Pontecorvi A, Boscaro M, Palù G. Modulation of retrovirally driven therapeutic genes by mutant *TP53* in anaplastic thyroid carcinoma. *Cancer Gene Ther* 2005;12(4):381–388.
21. Nagayama Y, Yokoi H, Takeda K, Hasegawa M, Nishihara E, Namba H, Yamashita S, Niwa M. Adenovirus-mediated tumor suppressor p53 gene therapy for anaplastic thyroid carcinoma in vitro and in vivo. *J Clin Endocrinol Metab* 2000;85(11):4081–4086.
22. Moretti F, Farsetti A, Soddu S, Misiti S, Crescenzi M, Filetti S, Andreoli M, Sacchi A, Pontecorvi A. p53 re-expression inhibits proliferation and restores differentiation of human thyroid anaplastic carcinoma cells. *Oncogene* 1997;14(6):729–740.